PHYSICAL REVIEW C VOLUME 37, NUMBER 5 MAY 1988

# Covariant approach to $\pi^+$-proton bremsstrahlung

R. Wittman
*TRIUMF, Vancouver, British Columbia, Canada V6T 2A3*
(Received 9 October 1987)

The pion-proton bremsstrahlung process is considered in a Δ-isobar model that treats the full Lorentz structure and off-shell nature of the Rarita-Schwinger spin-$\frac{3}{2}$ propagator and vertex functions. The relativistic isobar model necessarily produces background $S_{31}$, $P_{31}$, and $D_{33}$ partial waves as well as the resonant $P_{33}$ wave, but explicit background is needed to fit the elastic data. Unitarity and gauge invariance as well as the soft photon limit are preserved in the model. The $\pi^+$-p elastic and radiative processes are treated on the same dynamical footing within a relativistic $K$-matrix approach. The approach is constructed in a form that formally resembles a four-dimensional scattering theory to allow a more physical or intuitive illustration of the underlying dynamics.

## I. INTRODUCTION

With the pressing need for models of hadronic substructure and ultimately for quantum chromodynamics (QCD) to make contact with as many "well determined" observables as is possible, a continuing experimental[1–3] and theoretical[4,5] effort exists to extract the Δ(1232) diagonal as well as transition electromagnetic observables. For this reason, the original suggestion of Kondratyuk and Ponomarev[6] to consider radiative $\pi^+$p scattering as a means of deducing the diagonal $\Delta^{++}$ magnetic moment continues to encourage the refinement by bremsstrahlung measurements and the construction of phenomenological models that satisfy important theoretical constraints. Recently, the MIT model of Heller *et al.*[5] has become the first calculation (explicitly containing the Δ isobar) that respects gauge invariance, unitarity, and the soft photon limit as well as considers a dynamical treatment of the $\pi$NΔ vertex function. Their work stresses the need for dynamical consistency between the elastic and radiative processes—indeed the definition of a magnetic moment of a strongly decaying particle demands this consistency. Although this model stands alone in its theoretical soundness and in the detailed treatment of nonrelativistic $\pi$NΔ and Δ$\gamma$Δ vertex functions, one might consider a model containing these desirable theoretical features without the formal complications that arise when form factors are introduced. Also, it should be instructive to consider a model that retains Lorentz invariance and includes antiparticle intermediate states since relativistic approaches have proved fruitful[7] in describing other processes—especially when spin observables are involved. The model presented in this work may be considered as the simplest phenomenological approach available that respects gauge invariance, unitarity, the soft photon limit, and Lorentz invariance, while retaining a consistent link between bremsstrahlung and elastic scattering. It seems reasonable that such a model should be tested before (or along with) a model[5] that includes a detailed treatment of the strong and electromagnetic structure functions. Although the present approach is rooted in the effective Lagrangian procedure of other authors,[4] *such an approach is yet to be applied to the $\pi^+$p bremsstrahlung problem.* This is because unitarity is either absent or incomplete in other effective Lagrangian models[4] that introduce the Δ width in an *ad hoc* manner. In the present model both the Δ width and radiation by internal processes arise from dynamical origins within a relativistic $K$-matrix approach without the need of specifying the detailed dynamics of structure functions. Reasonable agreement between the present calculation and the cross section data obtained by Nefkens *et al.*[1] is found using $\mu_{\Delta^{++}}/\mu_p \approx 2.3$; it is seen in the figures that the full calculation results are very comparable to those of the MIT model. The present approach, although simpler in some respects to the MIT approach, allows the advantage of retaining the full covariant structure and frame independence of all expressions. Therefore, the boosting of amplitudes or of vertex functions is avoided. Also a partial wave decomposition of the amplitude is unnecessary to address the bremsstrahlung process. The price that one pays for this pedagogically simpler program is that the contractions of Lorentz and Dirac indices must be handled explicitly (numerically), and the four-dimensional structure of the Bethe-Salpeter equation must be retained at least to the point of providing unitarity and Lorentz invariance.

In Sec. II, the elastic $\pi^+$p scattering amplitude is constructed in a $K$-matrix approach and appears formally equivalent to the solution of a four-dimensional scattering equation. This organization of terms allows an intuitive path to the two-channel $K$-matrix version of the radiative amplitude. The bremsstrahlung amplitude is then given in detail in Sec. III. Contact is then made with the data to assess the validity of the model and to constrain what one would like to interpret as the "physical" $\Delta^{++}$ magnetic moment.

## II. ELASTIC $\pi^+$p SCATTERING

Since only $\pi^+$p scattering is considered, it is understood that all amplitudes correspond to the total isospin

 

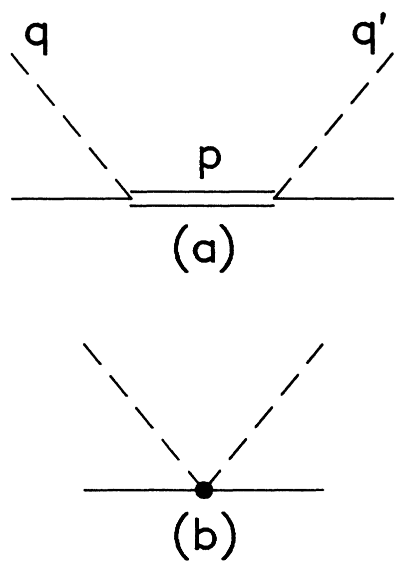


FIG. 1. Elastic scattering driving amplitudes: (a) The $\Delta$-isobar term labeling the incoming and outgoing pion (dashed lines) momenta and intermediate $\Delta$ (double line) momentum. The proton is denoted with solid lines. (b) The background term.

$\frac{3}{2}$ channel. The driving physics consists of the $\Delta(1232)$ term and a background term (Fig. 1). The $\Delta$ term follows from the interaction of the Rarita-Schwinger (RS) spin-$\frac{3}{2}$ field $[\Delta_\mu(x)]$, with the pion and nucleon fields according to

$$\mathcal{L}_{\pi N\Delta}=\frac{g_\Delta}{2m}\bar{\Delta}_\mu(x)\Theta^{\mu\nu}(Z)\mathrm{N}(x)\partial_\nu\pi(x)+\mathrm{H.c.}\ . \quad (1)$$

Since the relativistic off-mass-shell[8] spin-$\frac{3}{2}$ particle can propagate with $J^P=\frac{3}{2}^+$ or $\frac{1}{2}^+$, and antiparticle with $J^P=\frac{3}{2}^-$ or $\frac{1}{2}^-$, the $\pi N\Delta$ interaction [Eq. (1)] is allowed an off-shell freedom contained in the $Z$ parameter of the tensor defined by

$$\Theta^{\mu\nu}(Z)=g^{\mu\nu}-(Z+\tfrac{1}{2})\gamma^\mu\gamma^\nu\ . \quad (2)$$

This $Z$ parameter has the effect of varying the strength of the off-shell $\pi N\Delta$ coupling to the $J^P=\frac{1}{2}^+$ and $\frac{1}{2}^-$ channels, but has no effect on the resonance $J^P=\frac{3}{2}^+$ or the $J^P=\frac{3}{2}^-$ channels. A popular value for $Z$ in the literature is naturally $Z=-\frac{1}{2}$. Peccei[9] chooses $Z=-\frac{1}{4}$ in order that $\gamma\cdot\Theta^\mu(-\frac{1}{4})=0$, but there seems to be no theoretical bias for this choice. It should be noted that there is no value of $Z$ that can totally quench the $\pi N$ coupling to these lower spin off-shell $\Delta$ components. Extensive work has been devoted to the determination of $Z$ on theoretical[10] as well as phenomenological[11,12] grounds. In this work $Z$ is taken as an arbitrary parameter ($Z\approx-0.15$) along with the three other parameters to fit the background $S_{31}$ and $P_{31}$ partial wave phase shifts. The driving term for the $\Delta$ is then simply the Born amplitude for the graph of Fig. 1(a) and can be written as

$$\bar{u}_f V_\Delta u_i=\left[\frac{g_\Delta}{2m}\right]^2\bar{u}_f q'_\mu\Theta^{\mu\alpha}(Z)[H_{\Delta 0}^{-1}(p)]_{\alpha\beta}\Theta^{\beta\nu}(Z)q_\nu u_i\ , \quad (3)$$

where $u_i$ and $u_f$ are the initial and final Dirac spinors for the nucleon, $q^\mu$ and $q'^\mu$ are the initial and final pion four-momenta, $p^\mu$ is the total (or $\Delta$) four-momentum, $m$ is the proton mass, and $g_\Delta$ is the $\pi N\Delta$ coupling strength ($g_\Delta\approx 29.58$). Also,

$$H_{\Delta 0}^{\mu\nu}(\mathrm{p})=(-g^{\mu\nu}+\gamma^\mu\gamma^\nu)(\not{p}-M)+p^\mu\gamma^\nu-\gamma^\mu p^\nu \quad (4)$$

yields the commonly used (Peccei[9], $w=-1$) "free" RS propagator. In Eq. (4), $M$ is the $\Delta$-isobar mass ($M=1231.8$ MeV) and $\not{p}$ refers to the scalar product $p\cdot\gamma=p^\mu\gamma_\mu$, where the metric convention is that of Bjorken and Drell.[13]

Once the driving dynamics is defined, one still needs to account for the $\Delta$ decay width as well as the unitarity constraint between the real and imaginary part of the full amplitude while retaining manifest Lorentz invariance. One approach that fulfills these goals is to use $V_\Delta$ as a driving term in the Bethe-Salpeter equation

$$T_\Delta(p,q',q)=V_\Delta(p,q',q)+\int\frac{d^4k}{(2\pi)^4}V_\Delta(p,q',k)G(p,k)T_\Delta(p,k,q) \quad (5)$$

in order to sum a unitary set of graphs and thus, dynamically introduce the $\Delta$ width. Since $V_\Delta$ is separable, $T_\Delta$ can be found formally in the closed form

$$T_\Delta=\left[\frac{g_\Delta}{2m}\right]^2 q'_\mu\Theta^{\mu\alpha}(Z)[H_\Delta^{-1}(\mathrm{p})]_{\alpha\beta}\Theta^{\beta\nu}(Z)q_\nu\ , \quad (6)$$

where the full $\Delta$ propagator is derived from

$$H_\Delta^{\mu\nu}(\mathrm{p})=H_{\Delta 0}^{\mu\nu}(\mathrm{p})-\left[\frac{g_\Delta}{2m}\right]^2\Theta^{\mu\alpha}(Z)\Sigma_{\alpha\beta}(p)\Theta^{\beta\nu}(Z)\ . \quad (7)$$

The mass tensor $\Sigma$ [Fig. 2(a)] is given by

$$\Sigma^{\mu\nu}(\mathrm{p})=\int\frac{d^4k}{(2\pi)^4}k^\mu G(p,k)k^\nu\ , \quad (8)$$

where

$$G(p,k)=\frac{i}{k^2-\mu^2+i\epsilon}\,\frac{1}{\not{p}-\not{k}-m+i\epsilon}\ , \quad (9)$$

with $\mu$ as the pion mass. Clearly the real part of the above integral diverges without the introduction of a "reasonable" cutoff procedure. In order to avoid the complexity that can arise in the radiative sector when form factors are introduced, the real part of $\Sigma$ will not be calculated, but assumed to be included in the "physical" mass $M$. This prescription is nothing more than the $K$-matrix approach since only the imaginary part of $\Sigma$ is responsible for preserving two-body unitarity. This approach can be considered as a recipe for forcing unitarity, and it simply amounts to taking the real Born or tree level amplitude as the $K$-matrix or stationary wave solution for the amplitude. It should be confessed that with this prescription, $T_\Delta$ [Eq. (6)] is no longer a solution of the Bethe-Salpeter equation [Eq. (5)], yet the Lorentz invariance and unitarity properties are preserved. Although the following expressions may seem to be an unnecessarily formal representation of this method, they will prove useful in considering questions of unitarity and gauge invariance in the radiative case and will allow a physically intuitive path to the bremsstrahlung amplitude.

Although the relativistic isobar term implicitly produces background contributions, one cannot fit the background partial wave phase shifts by adjusting the $Z$ parameter alone. Therefore, the full driving potential must contain explicit background ($V=V_\Delta+V_B$). The background driving term [Fig. 1(b)] is taken to be

$$V_B=b_1 q'\cdot q+b_2\mu^2+b_3(\not{q}'+\not{q})+b_4\not{q}\not{q}' , \tag{10}$$

and can be considered as remnants of $\sigma$ exchange ($b_1,b_2$), $\rho$ exchange ($b_3$), and crossed nucleon ($b_4$) graphs from an ultrastatic reduction of internal dynamics, although the constants ($b_i$'s) do not necessarily follow directly from these assignments. $V_B$ can now formally be written in a separable form that appears similar to the $\Delta$ term as

$$V_B=q'^{\mu}[H_{B0}^{-1}]_{\mu\nu}q^{\nu} . \tag{11}$$

This is possible by adopting a convenient notation, where all the pion four momenta $q'^{\mu}$, $q^{\mu}$, and $k^{\mu}$ are considered to have a "fifth" ($\mu=4$) component which is a Lorentz

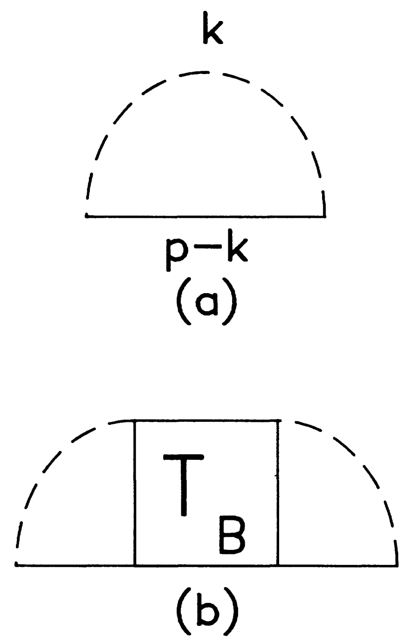


FIG. 2. (a) Representation of the mass tensor $\Sigma$ and (b) the additional background contribution to the $\Delta$ self energy.

scalar (i.e., $q'^{\mu}=q^{\mu}=k^{\mu}=1$), but *all* other Lorentz vectors (and tensors) which do not implicitly contain a pion four momenta (e.g., $g^{\mu\nu}$) are zero for this ($\mu=4$) component. Of course the upper and lower "fifth" components are equal. Also, $\delta^{\mu}$ defined as

$$\delta^{\mu}\equiv\begin{cases}0, & \mu=0,1,2,3\\ 1, & \mu=4\end{cases}$$

becomes a useful quantity since, for instance $H_{B0}^{\mu\alpha}[H_{B0}^{-1}]_{\alpha}^{\nu}=g^{\mu\nu}+\delta^{\mu}\delta^{\nu}$, where

$$H_{B0}^{\mu\nu}=\frac{1}{b_1+2b_4}g^{\mu\nu}+\frac{1}{\mu^2 b_2(b_1-2b_4)-4b_3^2}\left[\frac{\mu^2 b_2 b_4+b_3^2}{b_1+2b_4}\gamma^{\mu}\gamma^{\nu}+(b_1-2b_4)\delta^{\mu}\delta^{\nu}-b_3(\delta^{\mu}\gamma^{\nu}+\gamma^{\mu}\delta^{\nu})\right] . \tag{12}$$

The full elastic amplitude can now be expressed in the compact form

$$T\equiv q'^{\mu}[H^{-1}(p)]_{\mu\nu}q^{\nu} . \tag{13}$$

It is noted that, in the center-of-momentum frame, the amplitude $T$ is related to the traditional invariant amplitudes by

$$\bar{u}_f T u_i=-\bar{u}_f[A+\tfrac{1}{2}(\not{q}'+\not{q})B]u_i . \tag{14}$$

$[H^{-1}(\mathrm{p})]$ of Eq. (13) now contains both $\Delta$ and explicit background terms and can be given in a form that illustrates the role of both processes (suppressing the Lorentz indices):

$$H^{-1}(\mathrm{p})=H_B^{-1}(\mathrm{p})+\left[\frac{g_\Delta}{2m}\right]^2[g+H_B^{-1}(\mathrm{p})\Sigma(\mathrm{p})]\Theta(Z)H_\Delta^{-1}(\mathrm{p})\Theta(Z)[g+\Sigma(\mathrm{p})H_B^{-1}(\mathrm{p})] , \tag{15}$$

where $H_B^{-1}(\mathrm{p})$ is derived from

$$H_B(\mathrm{p})=H_{B0}-\Sigma(\mathrm{p}) , \tag{16}$$

and the full Δ propagator is now derived from

$$H_\Delta(\mathrm{p})=H_{\Delta 0}(\mathrm{p})-\left[\frac{g_\Delta}{2m}\right]^2\Theta(Z)[\Sigma(\mathrm{p})+\Sigma(\mathrm{p})H_B^{-1}(\mathrm{p})\Sigma(\mathrm{p})]\Theta(Z)\ , \tag{17}$$

which includes contributions from both processes of Fig. 2. Explicitly, the mass matrix is taken to be

$$\Sigma^{\mu\nu}(\mathrm{p})=\frac{i}{4\pi}\frac{q_s}{6\sqrt{s}}\left\{q_s^2\left[(\not p+m)g^{\mu\nu}-\frac{\omega_s}{\sqrt{s}}(g^{\mu\nu}\not p+p^\mu\gamma^\nu+\gamma^\mu p^\nu)\right]+\left[\frac{3\omega_s}{\sqrt{2}}(q_s^2+\omega_s^2)\not p-(q_s^2+3\omega_s^2)(\not p+m)\right]\frac{p^\mu p^\nu}{p\cdot p}\right\}$$
$$+\frac{i}{4\pi}\frac{q_s}{2\sqrt{s}}\left\{\left[\frac{\omega_s}{\sqrt{s}}\not p-(\not p+m)\right]\delta^\mu\delta^\nu-\tfrac{1}{3}q_s^2(\delta^\mu\gamma^\nu+\gamma^\mu\delta^\nu)+\left[\frac{q_s^2+3\omega_s^2}{3s}\not p-\frac{\omega_s}{\sqrt{s}}(\not p+m)\right](p^\mu\delta^\nu+\delta^\mu p^\nu)\right\}\ , \tag{18}$$

where the quantities $s$, $q_s$, and $\omega_s$ are introduced as shorthand for: $s=p\cdot p$,

$$\omega_s=\frac{s-m^2+\mu^2}{2\sqrt{s}}\ ,$$

and $q_s=(\omega_s^2-\mu^2)^{1/2}$. In the center-of-momentum frame, $q_s$ corresponds to magnitude of the initial or final pion three momentum and $\omega_s$ corresponds to the pion energy, but here, they can simply be considered as scalar functions of the invariant mass squared ($s$).

The seven parameters of the model are found to be

$g_\Delta=29.58$, $b_1=1.185\ \mathrm{fm}^3$

$M=1231.8$ MeV, $b_2=12.065\ \mathrm{fm}^3$

$Z=-0.146$, $b_3=-4.203\ \mathrm{fm}^2$

$b_4=3.724\ \mathrm{fm}^3$

where $g_\Delta$, $M$, and one combination of background parameters ($b_1+2b_4$) are adjusted to fit the resonant $P_{33}$ phase (Fig. 4). The pole position of this partial wave is found to be at $\sqrt{s}=1208-50.5i$ MeV, in fair agreement with the particle data group[14] value of $\sqrt{s}=1210\pm0.5-(50\pm1)i$ MeV. The remaining three background parameters and $Z$ are varied to fit the background $S_{31}$ and $P_{31}$ phases. Since the soft photon limit of the bremsstrahlung process follows directly from the elastic data, it is crucial that the elastic amplitude [Eq. (13)] can realistically make contact with the experimental phase shifts. Figures 3 and 4 compare the $S_{31}$, $P_{31}$, and resonant $P_{33}$ partial wave phase shifts projected from $T$ [Eq. (13)] above (dashed line) to be experimental[15] phase shifts (solid line). In Fig. 4 it is seen that the $P_{33}$ data can be fully reproduced in a relativistic $K$-matrix approach that includes a mild amount of background in the $P_{33}$ channel. This is noted in a similar approach by Olsson.[16] The fit to the background phases (Fig. 3) is perhaps less impressive because of the minimal amount of dynamics included in the background driving term [Eq. (10)]; the background phases can be trusted to within ≈10% through most of the energy region of interest. This can lead to only a few percent error in the elastic cross section and ≈10% error in the asymmetry.

## III. THE $\pi^+$p BREMSSTRAHLUNG AMPLITUDE

Using the machinery developed for the elastic amplitude, the construction of a covariant bremsstrahlung amplitude that can satisfy both unitarity (to order $e$) and gauge invariance requirements simply proceeds through considering *all* radiative processes to order $e$. This is clearly achieved by a sum of four terms (again suppressing the Lorentz indices):

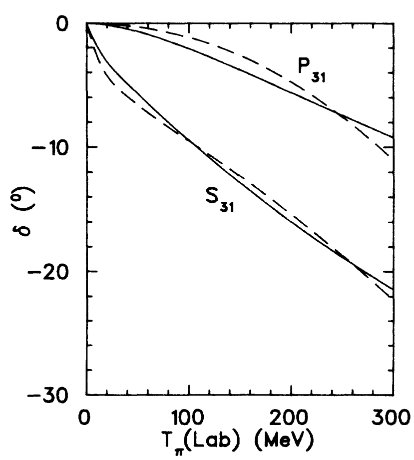


FIG. 3. The total isospin $\frac{3}{2}$ background $S$ and $P$ wave phase shifts, comparing the model calculation (dashed line) to the data (Ref. 15) (solid line).

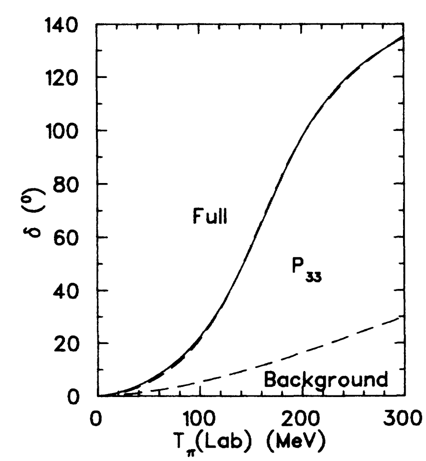


FIG. 4. The resonant $P_{33}$ partial wave phase shift showing the full amplitude result with the background contribution alone (legends are as in Fig. 3).

$$T_\gamma = R'\cdot\epsilon H^{-1}(\mathrm{p})q + q'H^{-1}(\mathrm{p}')R\cdot\epsilon + q'H^{-1}(\mathrm{p}')\Lambda(\mathrm{p}',\mathrm{p})\cdot\epsilon H^{-1}(\mathrm{p})q$$
$$+\left[\frac{g_\Delta}{2m}\right]^2 q'[g+H_B^{-1}(\mathrm{p}')\Sigma(\mathrm{p}')]\Theta(Z)H_\Delta^{-1}(\mathrm{p}')J_\Delta\cdot\epsilon H_\Delta^{-1}(\mathrm{p})\Theta(Z)[g+\Sigma(\mathrm{p})H_B^{-1}(\mathrm{p})]q\ , \qquad (19)$$

where the first two terms concisely account for all radiation by the external legs, and explicitly contain

$$R^\mu\cdot\epsilon = q^\mu \frac{1}{\not p' - \not q - m}\left[e_{\mathrm{N}}\not\epsilon + \frac{\kappa_{\mathrm{N}}}{4m}(\not\epsilon\not\nu - \not\nu\not\epsilon)\right]$$
$$-(q^\mu - \nu^\mu)e_\pi \frac{q\cdot\epsilon}{q\cdot\nu} - e_\pi\epsilon^\mu \qquad (20)$$

and

$$R'^\mu\cdot\epsilon = \left[e'_{\mathrm{N}}\not\epsilon + \frac{\kappa'_{\mathrm{N}}}{4m}(\not\epsilon\not\nu - \not\nu\not\epsilon)\right]\frac{1}{\not p - \not q' - m}q'^\mu$$
$$+e'_\pi \frac{q'\cdot\epsilon}{q'\cdot\nu}(q'^\mu + \nu^\mu) - e'_\pi\epsilon^\mu\ , \qquad (21)$$

with $p^\mu$ and $p'^\mu$ as the initial and final total pion-nucleon four-momenta, $\nu^\mu$ ($\nu^\mu = p^\mu - p'^\mu$) and $\epsilon^\mu$ as the photon four-momentum and polarization, $e_{\mathrm{N}}$ and $e_\pi$ as the nucleon and pion charges (e.g., $e_{\mathrm{p}}=1$, $e_{\pi^+}=1$), and $\kappa_{\mathrm{N}}$ the anomalous nucleon magnetic moment ($\kappa_{\mathrm{p}}\approx 1.79$). The last term of Eq. (19) is the direct $\Delta(1232)$ radiation contribution containing the $\Delta$ current (Fig. 5)

$$J_\Delta^{\mu\nu}\cdot\epsilon = e_\Delta[(-g^{\mu\nu} + \gamma^\mu\gamma^\nu)\not\epsilon + \epsilon^\mu\gamma^\nu - \gamma^\mu\epsilon^\nu]$$
$$-g^{\mu\nu}\frac{\kappa_\Delta}{4m}(\not\epsilon\not\nu - \not\nu\not\epsilon)\ , \qquad (22)$$

where the first term of Eq. (22) follows from a minimal substitution $p^\mu \to p^\mu - e_\Delta\epsilon^\mu$ on $H_{\Delta 0}(\mathrm{p})$ [Eq. (4)]; the second term provides the anomalous $\Delta$ magnetic moment. Therefore, the $\Delta$ magnetic moment, in soft photon limit, and in the $\Delta$ rest frame is given according to

$$\frac{\mu_{\Delta^{++}}}{\mu_{\mathrm{p}}} \to \frac{2m/M + \kappa_{\Delta^{++}}}{1+\kappa_{\mathrm{p}}}\ ; \qquad (23)$$

it is noted that the static SU(6) quark model, for instance, predicts a value of 2 for this ratio. Here, the ratio $\mu_{\Delta^{++}}/\mu_{\mathrm{p}}$ becomes the only free parameter when addressing the radiative observables. This can be considered a very conservative approach since the relativistic $\Delta\gamma\Delta$ vertex contains a rich Lorentz structure[8] allowing a number of independently gauge invariant couplings (not only the higher electromagnetic moments, i.e., $E2$ and $M3$) both on and off-mass-shell. Naturally, these additional couplings reflect uncertainty in the present model and will be considered at a later date.

The third term of Eq. (19) includes all radiation from the internally propagating charged pion and nucleon lines (Fig. 6), where $\Lambda^{\mu\nu}(\mathrm{p}',\mathrm{p})\cdot\epsilon$ can be considered the simplest vertex correction to $J^{\mu\nu}\cdot\epsilon$, thus gauge invariance is exhibited through the Ward identity

$$\Lambda^{\mu\nu}(\mathrm{p}',\mathrm{p})\cdot(\mathrm{p}-\mathrm{p}') = (e_\pi + e_{\mathrm{N}})[\Sigma^{\mu\nu}(\mathrm{p}') - \Sigma^{\mu\nu}(\mathrm{p})]\ . \qquad (24)$$

Actually, it is sufficient that this Ward identity [Eq. (24)] be satisfied to have current conservation for the entire bremsstrahlung amplitude [Eq. (19)], although it is still a tedious exercise to show that the amplitude vanishes with the replacement $e^\mu \to \nu^\mu$. A numerical verification of current conservation is made for each point calculated in Figs. 7–14 cited in Sec. IV. The internal current of Fig. 6 can be written literally as

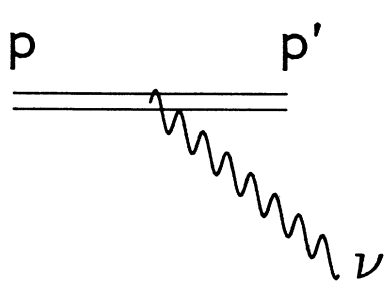


FIG. 5. The direct Δ radiation vertex.

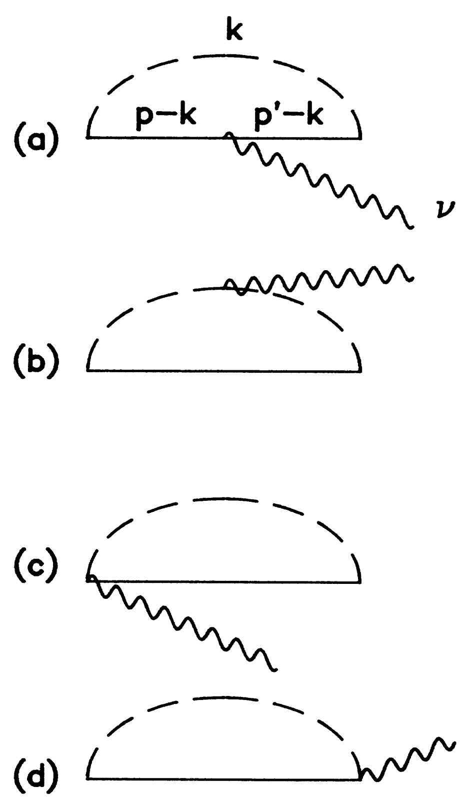


FIG. 6. Representation for internal (a) nucleon, (b) pion, and (c) and (d) contact radiation processes.

$$\Lambda^{\mu\nu}(\mathrm{p}',\mathrm{p})\cdot\epsilon=i\int\frac{d^4k}{(2\pi)^4}\left\{k^\mu\frac{1}{k^2-\mu^2+i\epsilon}\frac{1}{\not p'-\not k-m+i\epsilon}\left[e_{\mathrm{N}}\not\epsilon+\frac{\kappa_{\mathrm{N}}}{4m}(\not\epsilon\not v-\not v\not\epsilon)\right]\frac{1}{\not p-\not k-m+i\epsilon}k^\nu\right.$$

$$+(k^\mu-v^\mu)\frac{1}{(k-v)^2-\mu^2+i\epsilon}e_\pi(2k-v)\cdot\epsilon\frac{1}{k^2-\mu^2+i\epsilon}\frac{1}{\not p-\not k-m+i\epsilon}k^\nu$$

$$\left.-e_\pi\epsilon^\mu\frac{1}{k^2-\mu^2+i\epsilon}\frac{1}{\not p-\not k-m+i\epsilon}k^\nu-k^\mu\frac{1}{k^2-\mu^2+i\epsilon}\frac{1}{\not p'-\not k-m+i\epsilon}e_\pi\epsilon^\nu\right\} \quad (25)$$

and once again it is noted that the real part of the integral diverges. It is therefore consistent with the $K$-matrix approach and with the Ward identity [Eq. (24)] to calculate only the imaginary part of $\Lambda^{\mu\nu}(\mathrm{p}',\mathrm{p})\cdot\epsilon$. The real part is effectively included in the direct $\Delta$ current of Fig. 5, which is now considered to be the "physical" current. The imaginary part of $\Lambda^{\mu\nu}(\mathrm{p}',\mathrm{p})\cdot\epsilon$ can readily be found by setting internal pion and nucleon lines of Fig. 6 on their positive-energy mass shells.[17] This is done by replacing propagators of the respective particles according to

$$(k^2-\mu^2+i\epsilon)^{-1}[(p-k)^2-m^2+i\epsilon]^{-1}\to-2\pi^2\delta(k^2-\mu^2)\theta(k^0)\delta((p-k)^2-m^2)\theta(p^2-k^0)\ . \quad (26)$$

Since the $\int k^2dk\int dk^0$ integral is done by the $\delta$ functions, an integral over solid angle remains and is given here in an arbitrary frame as

$$\Lambda^{\mu\nu}(\mathrm{p}',\mathrm{p})\cdot\epsilon=\frac{i}{4\pi}\int\frac{d\Omega_k}{8\pi}|\mathbf{k}|^3\left\{k^\mu\frac{\not p'-\not k+m}{2(p-k)\cdot v}\left[e_{\mathrm{N}}\not\epsilon+\frac{\kappa_{\mathrm{N}}}{4m}(\not\epsilon\not v-\not v\not\epsilon)\right]+(k^\mu-v^\mu)e_\pi\frac{k\cdot\epsilon}{k\cdot v}+e_\pi\epsilon^\mu\right\}\frac{\not p-\not k+m}{p^0|\mathbf{k}|^2-k^0\mathbf{p}\cdot\mathbf{k}}k^\nu$$

$$-\frac{i}{4\pi}\int\frac{d\Omega_{k'}}{8\pi}|\mathbf{k}'|^3k'^\mu\frac{\not p'-\not k'+m}{p'^0|\mathbf{k}'|^2-k'^0\mathbf{p}'\cdot\mathbf{k}'}\left\{\left[e_{\mathrm{N}}\not\epsilon+\frac{\kappa_{\mathrm{N}}}{4m}(\not\epsilon\not v-\not v\not\epsilon)\right]\frac{\not p-\not k'+m}{2(p'-k')\cdot v}k'^\nu\right.$$

$$\left.+e_\pi\frac{k'\cdot\epsilon}{k'\cdot v}(k'^\nu+v^\nu)-e_\pi\epsilon^\mu\right\}\ . \quad (27)$$

It should be noted that the magnitude $|\mathbf{k}|$ of the internal pion momentum and pion energy $k^0$ acquire angular dependence when expressed in an arbitrary frame as

$$|\mathbf{k}|=\frac{\sqrt{s}\,\omega_s(\mathbf{p}\cdot\hat{\mathbf{k}})+p^0[s\omega_s^2-\mu^2p^{02}+\mu^2(\mathbf{p}\cdot\hat{\mathbf{k}})^2]^{1/2}}{p^{02}-(\mathbf{p}\cdot\hat{\mathbf{k}})^2},\quad k^0=(|\mathbf{k}|^2+\mu^2)^{1/2} \quad (28)$$

with corresponding relations for $|\mathbf{k}'|$ and $k'^0$. As noted, the current of Eq. (27) does not add to the real part of the $\Delta$ magnetic moment, but it does lead to a static imaginary contribution of about $\mu_{\Delta^{++}}^{\mathrm{eff}}/\mu_{\mathrm{p}}=1.497i$; this is more than twice the value obtained in Ref. 5. Assuming charge symmetry, the soft photon limit contribution of Figs. 6(a) and (b) to the imaginary part of the $\Delta$ magnetic moment can be given in general according to

$$\mathrm{Im}\mu_\Delta^{\mathrm{eff}}=\frac{e}{4\pi}\left[\frac{g_\Delta}{2m}\right]^2\frac{q_s}{36M^3}\left[T_3[(4q_s^2+3E^2)E+(4q_s^2+3m^2)m]\right.$$

$$+\frac{3+T_3}{2}[2\omega_sq_s^2-\tfrac{9}{2}\omega_s(q_s^2+\omega_s^2)+(M+m)(q_s^2+3\omega_s^2)+\tfrac{3}{2}\omega_s(M+m)^2]$$

$$+\frac{M}{2m}\left[\frac{3+T_3}{2}\kappa_p\frac{3-T_3}{2}\kappa_n\right][2\omega_sq_s^2+3\omega_s(q_s^2+\omega_s^2)$$

$$\left.-2(M+m)(q_s^2+3\omega_s^2)+3\omega_s(M+m)^2]\right]\ , \quad (29)$$

where $T_3$ is twice the third component of the $\Delta$ isospin, and $E=M-\omega_s$. Since $v^\mu\to 0$, $\omega_s$ and $q_s$ in Eq. (29) are calculated for $\sqrt{s}=M$. Equation (29) should be independent of any vertex form factors that might be introduced, since all particles are on-mass-shell in this limit.

## IV. RESULTS

Here the model will be tested by comparing the calculated cross sections to the data of Ref. 1; the corresponding target asymmetries also will be shown. The differential cross section for the bremsstrahlung process can be written in terms of the amplitude given in Eq. (19) (in an arbitrary frame) as

$$\frac{d^3\sigma}{d\Omega_\pi d\Omega_\gamma d\nu^0} = \frac{|\mathbf{q}|\,|\mathbf{q}'|^3\,|\nu|\,m^2\alpha}{4(2\pi)^4(p^0|\mathbf{q}|^2-q^0\mathbf{p}\cdot\mathbf{q})(p'^0|\mathbf{q}'|^2-q'^0\mathbf{p}'\cdot\mathbf{q}')} \times\sum_{\epsilon}\tfrac{1}{2}\mathrm{Tr}\,|\bar{u}_f T_\gamma u_i|^2\,, \tag{30}$$

where $\alpha$ is the fine structure constant ($\alpha\approx\frac{1}{137}$). Also, the target polarization asymmetry ($A$) is defined as the ratio of the difference between the differential cross sections measured for spin-up and spin-down targets to sum; up and down refer to the direction of target spin with respect to the $\pi$N scattering plane. It is noted that in the figures to follow, the outgoing pion angle is assumed to be at a fixed value of $\alpha_\pi=50.5°$ with respect to the beam, and the same labeling as Ref. 1 for the outgoing pion and photon angles is used; the $\alpha$'s are the angles measured "clockwise" from the beam in the $\pi$N scattering plane and the $\beta$'s are the angles measured from the scattering plane to the normal. Figures 7 and 8 show the full coplanar photon angular distribution of cross section and asymmetry at two incident pion energies and two photon energies. The gross features of the calculated cross sections are in close agreement with the data and it will be seen that the bulk of Nefkens' data seems to be consistent with the present calculation. The curves of Figs. 7 and 8 correspond to three values of the $\Delta^{++}$ magnetic moment given by $\mu_{\Delta^{++}}/\mu_p=2.0$ (long dashed line), $\mu_{\Delta^{++}}/\mu_p=2.3$ (solid line) and $\mu_{\Delta^{++}}/\mu_p=2.7$ (short dashed line); at the larger photon energy the asymmetries are seen to be more

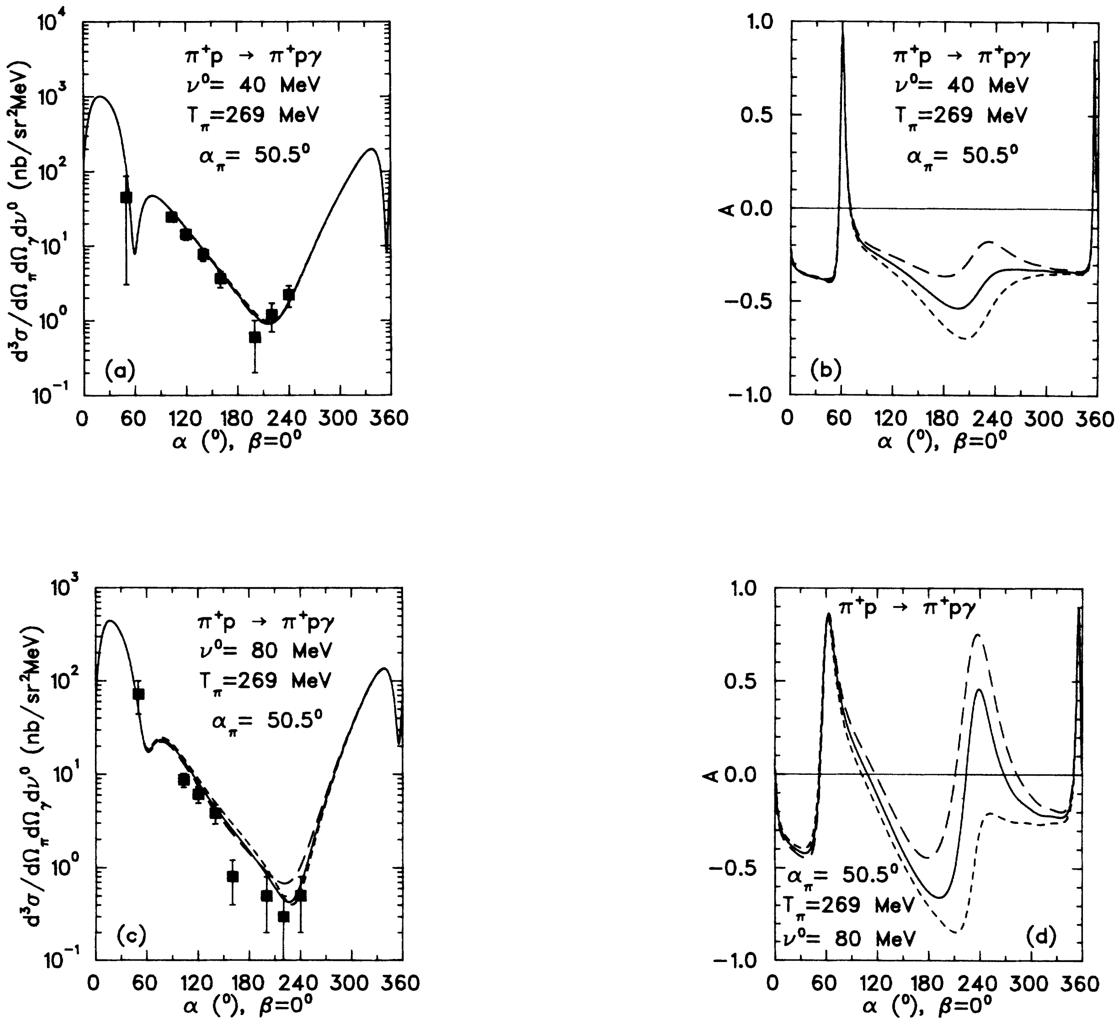


FIG. 7. The full coplanar photon angular distribution at $T_\pi=269$ MeV of (a) and (c) differential cross section and (b) and (d) proton polarization asymmetry for two photon energies. The curves correspond to calculations of the present model using the three values of the ratio $\mu_{\Delta^{++}}/\mu_p$: 2.0 (long dashed line), 2.3 (solid line), and 2.7 (short dashed line). The data is from Ref. 1.

distinct [Figs. 7(d) and 8(d)]. As in the MIT model, the calculated proton polarization asymmetry can show a strong sensitivity to $\mu_{\Delta^{++}}$; it is no surprise that the strongest sensitivity is found approximately near the SIN geometry,[2] where the photon angle is $\approx 240°$ and $T_\pi = 298$ MeV. Since the asymmetry (away from the elastic limit) can be very sensitive to the $\Delta^{++}$ magnetic moment, it is hoped that future asymmetry measurements,[3] in addition to the SIN measurement,[2] can provide a testing ground in determining the validity of applying model calculations in extracting this magnetic moment.

A more revealing test of the present calculation is seen in the photon spectra (Figs. 9 and 10) at two incident pion energies and four coplanar photon angles where there is only a mild sensitivity to $\mu_{\Delta^{++}}$. This region can provide a benchmark for the calculation because the $\Delta^{++}$ magnetic moment is the only free parameter of the model. Here, a very constrained prediction for the calculation is obtained, and it is preferable that any model that claims to extract $\mu_{\Delta^{++}}$ from the bremsstrahlung data should first prove reliable in $\mu_{\Delta^{++}}$ insensitive kinematical regions. Figures 9 and 10 show that a reasonable agreement is still found between the theory and experiment with the exception of the 160° photon angle data at higher ($\nu^0 \geq 60$ MeV) photon energies [Figs. 9(a) and 10(a)]. It is hoped that these minor differences can be absorbed into the uncertainties in the data and in the model without effecting the predictions of the model for the $\mu_{\Delta^{++}}$ sensitive cases. Clearly, additional cross section and asymmetry measurements in (theoretically) less sensitive regions, as well as experiments explicitly designed to measure $\mu_{\Delta^{++}}$,[2] will be valuable.

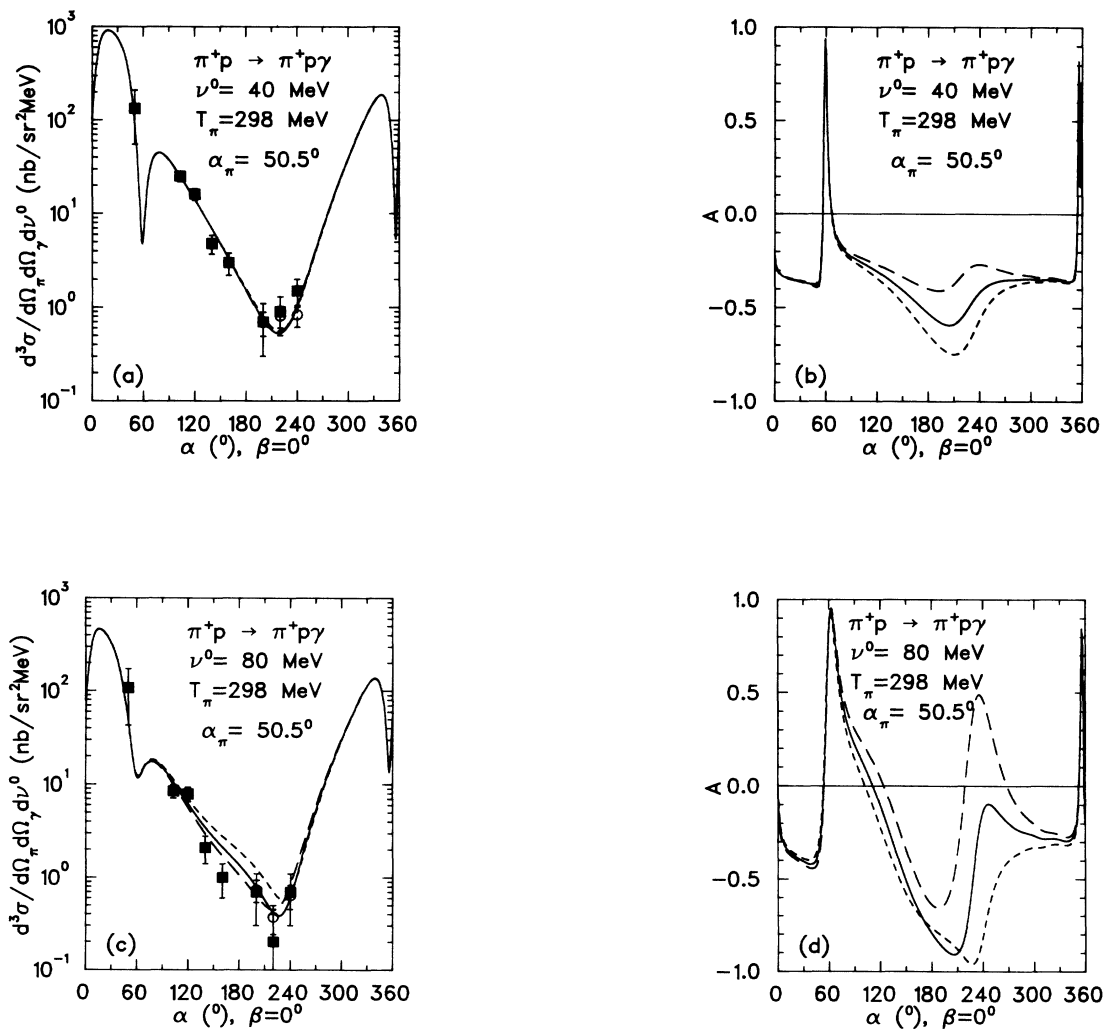


FIG. 8. The full coplanar photon angular distribution at $T_\pi = 298$ MeV for two photon energies. The curves and data are as in Fig. 7.

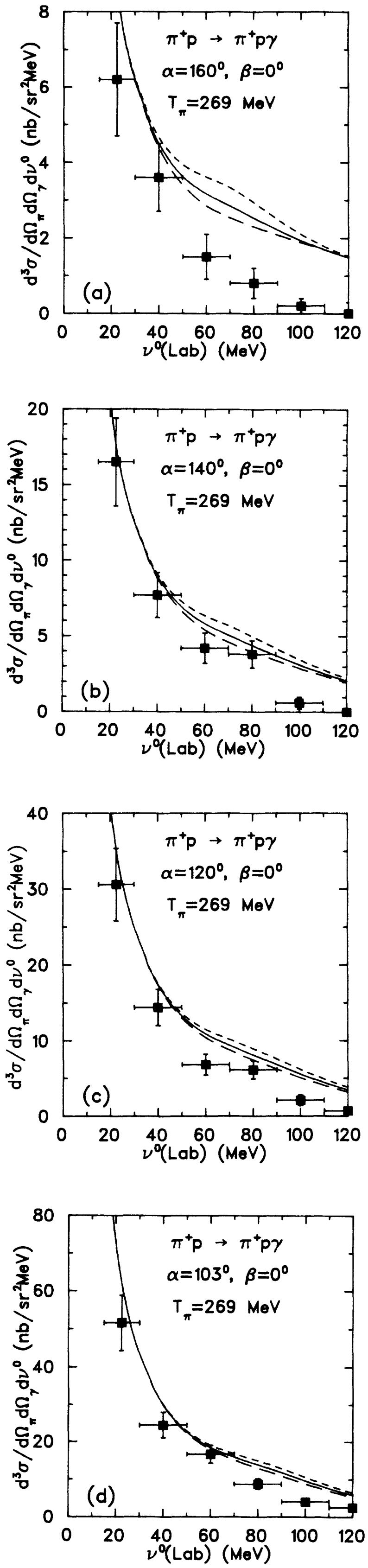


FIG. 9. The coplanar bremsstrahlung cross section at $T_\pi = 269$ MeV, shown for photon angles where only a mild sensitivity to $\mu_{\Delta^{++}}$ appears. The curves and data are as in Fig. 7.

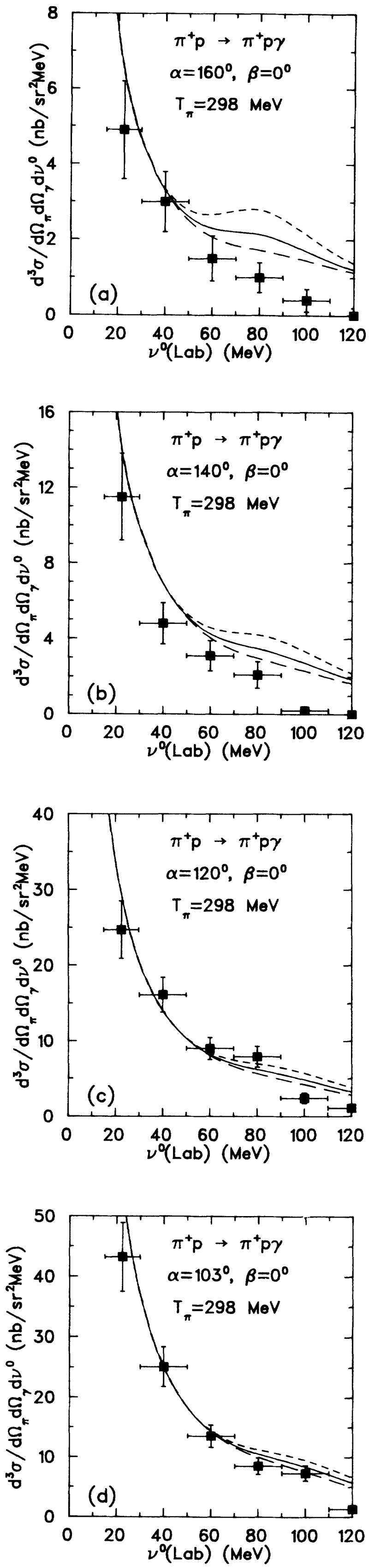


FIG. 10. Same as Fig. 9, but at $T_\pi = 298$ MeV. The curves and data are as in Fig. 7.

In considering the region that shows strongly sensitivity to $\mu_{\Delta++}$, six photon angles and two incident pion energies are considered (Figs. 11 and 12 ) to provide some overlap with Ref. 5. The same values of $\mu_{\Delta++}$ used in Figs. 7 and 8 are used in Figs. 11 and 12, where the data is consistent with the range $2.0 \leq \mu_{\Delta++}/\mu_p \leq 2.7$ with slight bias toward $\mu_{\Delta++}/\mu_p \approx 2.3$ (solid line). This is comparable to the "dressed' value $\tilde{\mu}_{\Delta++}/\mu_p \approx 2.5$ for the MIT model,[5] although such a simple comparison between these two different models may be misleading. For Fig. 12(a), the "Δ bump" will begin to appear for the larger value of $\mu_{\Delta++}$ (short dashed line); it can be shown that a strong cancellation between external and internal radiation continues to be the mechanism for suppressing this bump—although, it should be noted that this is *not* a gauge invariant separation. Additional asymmetry calcu-

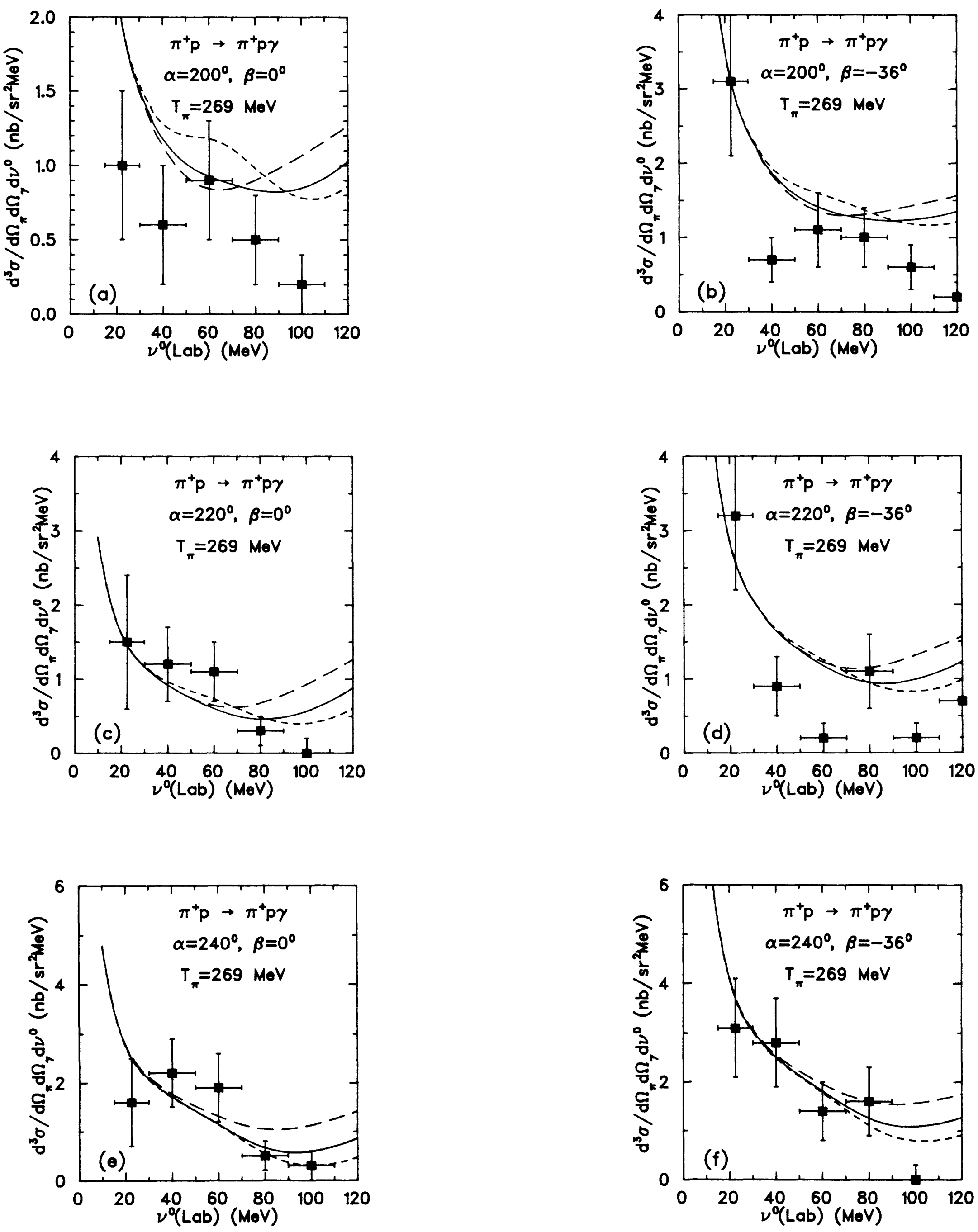


FIG. 11. Both coplanar and non-coplanar bremsstrahlung cross sections at $T_\pi = 269$ MeV, showing the sensitivity to $\mu_{\Delta++}$. The curves and data are as in Fig. 7.

lations are provided in Figs. 13 and 14 for photon angles that seem to show the greatest $\mu_{\Delta^{++}}$ sensitivity at these two outgoing pion energies. Fig. 13(a) shows that, even at the lower pion energy ($T_\pi = 269$ MeV), the asymmetry can vary dramatically for different values of $\mu_{\Delta^{++}}$.

The presentation of this model has tried to provide: (1) clarity for the underlying dynamics and (2) a comparison with many observables. Although the three-body final state leads to a vast number of observables,[18] it is hoped that the calculations provided in this work will allow the reader to judge the soundness of the model, and to make comparisons with other predictions regarding $\mu_{\Delta^{++}}$ sensitivity. Other kinematical geometries are presently being considered.[3]

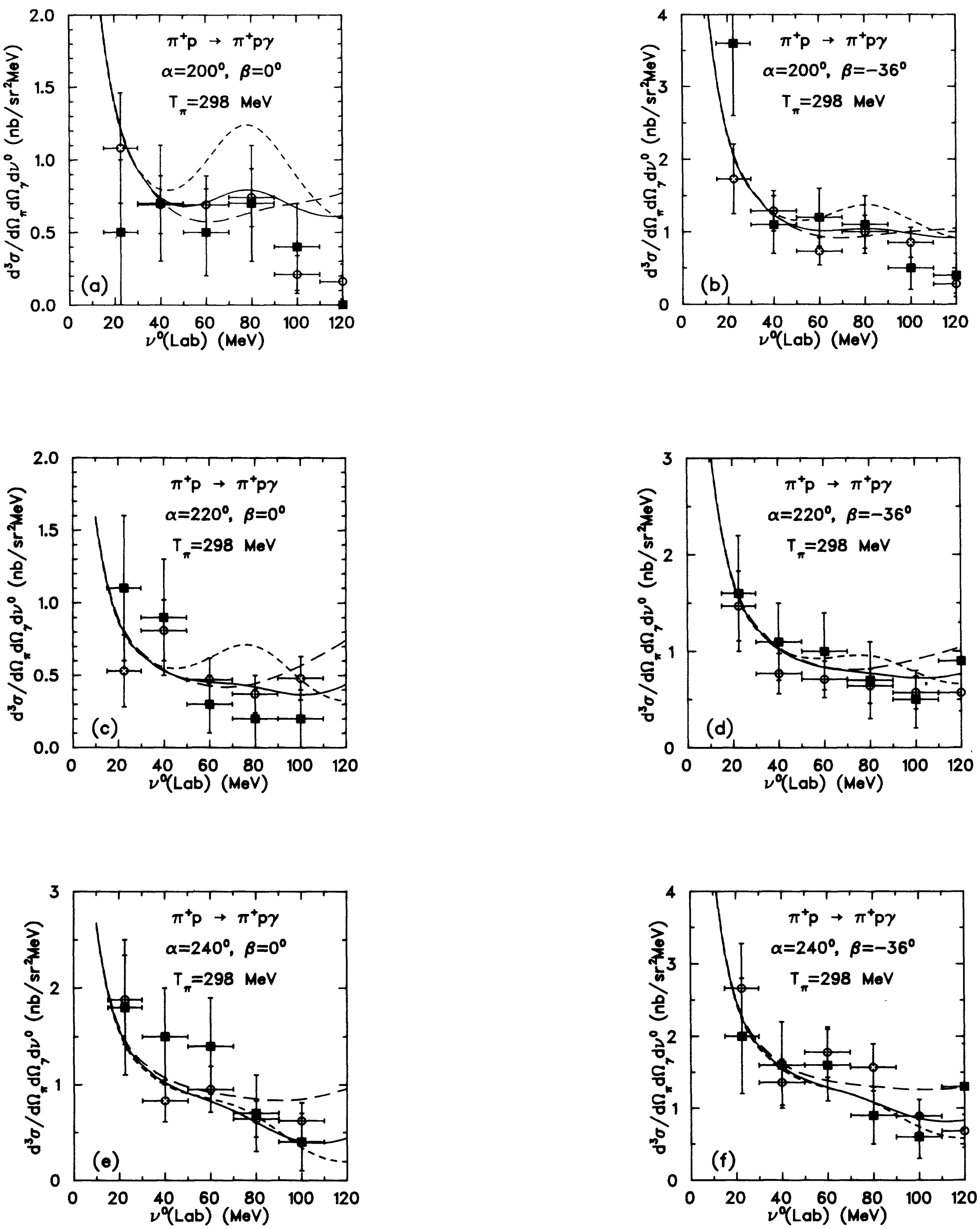


FIG. 12. Same as Fig. 11, but at $T_\pi = 298$ MeV. The curves and data are as in Fig. 7.

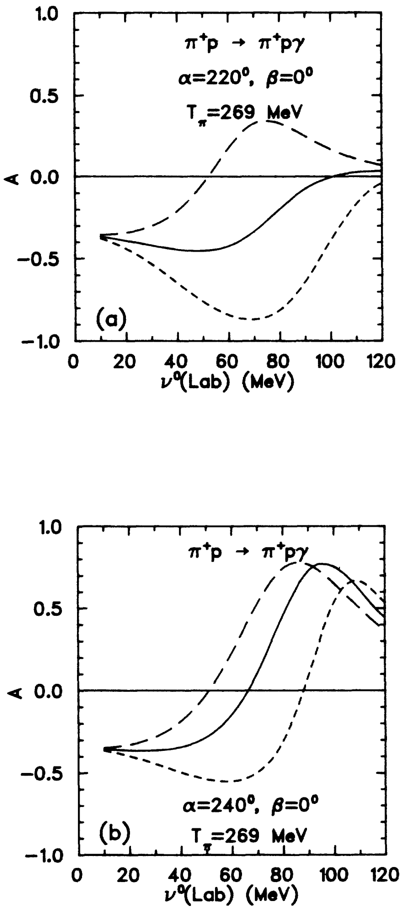


FIG. 13. Coplanar proton polarization asymmetry at $T_\pi=269$ MeV, showing a strong sensitivity to $\mu_{\Delta^{++}}$. These asymmetries correspond to the cross sections of Figs. 11(c) and (e). The legends for the curves are as Fig. 7.

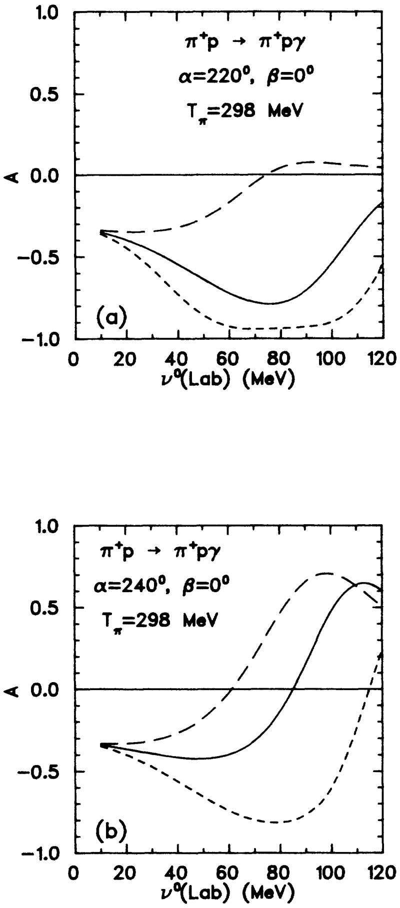


FIG. 14. Same as Fig. 13, but at $T_\pi=298$ MeV, and the asymmetries correspond to the cross sections of Figs. 12(c) and (e). The legends for the curves are as Fig. 7.

## V. CONCLUSION

It has been shown that a dynamically consistent model for the $\pi^+$p bremsstrahlung process can be constructed in a relativistic $K$-matrix approach. This model goes beyond the early phenomenological Lagrangian models by keeping the unitarity relationship between the elastic and radiative processes. An excellent fit to the elastic data is obtained by including explicit background modifications to the relativistic isobar amplitude. A reasonable amount of background is present in the $P_{33}$ channel,[16] although a model independent separation of background and $\Delta$ processes is not possible. The $\pi^+$p bremsstrahlung cross section data of Ref. 1 is found to agree with the present calculation over a wide range of kinematical conditions with the exception of the $\alpha=160°$ photon angle. Also, at $T_\pi=269$ MeV, the calculated cross sections seem to be consistently larger than the data at higher photon energies in the $\mu_{\Delta^{++}}$ sensitive region [Figs. 11(a)–(c)]. The data in this region at $T_\pi=269$ and 298 MeV is essentially consistent with a parameter range of $4.0 \le \kappa_{\Delta^{++}} \le 6.0$, for the $\Delta^{++}$ anomalous magnetic moment. The range $2.0 \le \mu_{\Delta^{++}}/\mu_p \le 2.7$ is then obtained from Eq. (23) for the effective magnetic moment ratio. The overall agreement between the data and the calculation presented here appears to be consistently as good as the MIT model of Ref. 5.

In principle, this approach can be naturally extended to the full scattering theory by introducing vertex form factors and carrying through the dispersive parts of the corresponding integrals. This may be necessary for a cleaner distinction between the magnetic moment obtained from the $\Delta$ and from the background processes. It would be interesting to consider if the gauge preserving currents of Ref. 5 could be obtained in such an approach.

## ACKNOWLEDGMENTS

The author is grateful for valuable discussions with D. S. Beder, T. Draper, H. W. Fearing, P. Fuchs, L. Heller, B. K. Jennings, S. Kumano, N. C. Mukhopadhyay and R. M. Woloshyn. This work is supported in part by the National Sciences and Engineering Research Council of Canada.

[1]B. M. K. Nefkens, M. Arman, H. C. Ballagh, Jr., P. F. Glodis, R. P. Haddock, K. C. Leung, D. E. A. Smith, and D. I. Sober, Phys. Rev. D **18**, 3911 (1978).

[2]P. Truöl *et al.,* SIN proposal; C. A. Meyer, Doctoral Dissertation, University of California, Berkeley, 1987.

[3]A. Stetz and P. Kitching, TRIUMF proposal for Experiment 446; and P. Fuchs, private communication.

[4]S. Baier, L. Pittner, and P. Urban, Nucl. Phys. **B27**, 589 (1971); D. S. Beder, *ibid.* **B84**, 362 (1975); P. Pascual and R. Tarrach, *ibid.* **B134**, 133 (1978); C. Picciotto, Phys. Rev. D **19**, 3244 (1979).

[5]L. Heller, S. Kumano, J. C. Martinez, and E. J. Moniz, Phys. Rev. C **35**, 718 (1987).

[6]A. Kondratyuk and L. A. Ponomarev, Yad. Fiz. **7**, 111 (1982) [Sov. J. Nucl. Phys. **7**, 82 (1968)].

[7]J. A. McNeil, J. R. Shepard, and S. J. Wallace, Phys. Rev. Lett. **50**, 1439 (1983); J. R. Shepard, J. A. McNeil, and S. J. Wallace, *ibid.* **50**, 1443 (1983).

[8]H. W. Fearing, G. R. Goldstein, and M. J. Moravcsik, Phys. Rev. D **29**, 2612 (1984).

[9]R. D. Peccei, Phys. Rev. **176**, 1812 (1968).

[10]L. M. Nath, B. Etemadi, and J. D. Kimel, Phys. Rev. D **3**, 2153 (1971).

[11]M. G. Olsson, Leaf Turner, and E. T. Osypowski, Phys. Rev. D **7**, 3444 (1973).

[12]M. G. Olsson and E. T. Osypowski, Nucl. Phys. **B87**, 366 (1975).

[13]J. D. Bjorken and S. D. Drell, *Relativistic Quantum Mechanics* (McGraw-Hill, New York, 1964).

[14]Particle Data Group, Review of Particle Properties, Phys. Lett. **170B**, 254 (1986).

[15]R. A. Arndt and L. D. Roper, scattering analyses interactive dial-in (SAID program) from Virginia Polytechnic Institute and State University, SP87 solution.

[16]M. G. Olsson, Nucl. Phys. **B78**, 55 (1974).

[17]S. Mandelstam, Phys. Rev. **115**, 1741 (1959); R. Cutkosky, J. Math. Phys. **1**, 429 (1960); S. D. Drell and H. R. Pagels, Phys. Rev. **140**, B397 (1965).

[18]M. Moravcsik and G. Goldstein, Phys. Rev. C **34**, 1411 (1986).